

Rapid Communication

Cite this article: Martín-Ramos P, Gil FC, Martín-Gil FJ, and Martín-Gil J. (2019) Characterization of exogenic fulgurites from an archaeological site in Tiedra, Valladolid, Spain. *Geological Magazine* **156**: 1455–1462. <https://doi.org/10.1017/S0016756819000438>

Received: 30 November 2018

Revised: 1 April 2019

Accepted: 4 April 2019

First published online: 17 May 2019





Keywords:

cristobalite; exofulgurite; keraunology; lightning strike; naquite; piroxenes; shocked quartz; Valladolid; Spain

Author for correspondence:

Pablo Martín-Ramos, Email: pmr@unizar.es

Characterization of exogenic fulgurites from an archaeological site in Tiedra, Valladolid, Spain

Pablo Martín-Ramos^{1,2,*} , Francisco PSC Gil² , Francisco J Martín-Gil¹  and Jesús Martín-Gil³ 

¹EPS, Instituto Universitario de Investigación en Ciencias Ambientales de Aragón (IUCA), University of Zaragoza, Carretera de Cuarte, s/n, 22071 Huesca, Spain; ²CFisUC, Physics Department, University of Coimbra, Rua Larga, P-3004-516, Coimbra, Portugal and ³Agriculture and Forestry Engineering Department, ETSIIAA, Universidad de Valladolid, Avenida de Madrid 44, 34004 Palencia, Spain

Abstract

Studies on type-V fulgurites are very sparse in the literature. This work reports on the characterization of natural exogenic fulgurites found at the archaeological site of Cerro de la Ermita (Tiedra, Valladolid, Spain), which was firstly a Celtiberian and then a Roman *locum sacrum*. Data from X-ray powder diffraction, X-ray fluorescence spectroscopy, Fourier-transform infrared spectroscopy and Raman spectroscopy suggest that the fulgurites consist of naquite, piroxenes, iron oxides, shocked quartz and neo-formed cristobalite.

1. Introduction

Fulgurites (from the Latin *fulgur*, meaning *thunderbolt*) are natural hollow glass tubes formed in silica, quartzose sand, rocks or soil by lightning strikes. They are formed when temperatures above 1800 °C, originating from a lightning bolt, instantaneously melt silica and other soil minerals on a conductive surface and grains are fused together; the fulgurite tube is the cooled product. This process occurs over a short period (c. 1 s), and leaves evidence of the lightning path and its dispersion over the surface. Fulgurites are usually formed in the topsoil and do not typically extend deeper than 40 cm into the less conductive subsoil. Instead, they run parallel to the surface of the ground (Carter *et al.*, 2010a). However, in some cases, fulgurites can be several metres deep (Martin Crespo *et al.*, 2009).

They are identified as a variety of the mineraloid lechatelierite (an amorphous form of silicon dioxide, SiO₂), although their absolute chemical composition is dependent on the physical and chemical properties of the soil (Gailliot, 2016; Elmi *et al.*, 2017). Their classification has generally been limited to varieties that are formed below the surface of the ground, such as soil, rock, sand or clay fulgurites (Pasek *et al.*, 2012). Occurrences of rock fulgurites associated with steel pylons of overhead electric transmission lines have also been reported (Kassi *et al.*, 2013).

In contrast, exogenic fulgurites, also referred to as ‘droplet fulgurites’ or as ‘type V’ fulgurites, are a fairly new concept. This class of fulgurites refers to liquefied materials resulting from a powerful lightning strike (>100 GW) that are thrown into the atmosphere above the lightning’s point of impact (i.e. they are ejected) and solidify in the air. Exogenic fulgurites feature an amorphous and often bubbly appearance due to the rapid manner in which the airborne, liquefied materials cool down. They are generally dark green in colour (as a result of a moderate iron oxide content), differing from traditional fulgurites, which are typically carrot, brown or tan. In addition, they have a smoother, glassier texture than conventional fulgurites, which have a gritty, sandy feel to them (Pasek *et al.*, 2012).

Although there are descriptions of fulgurites dating from the 12th century (such as the quartzofeld-spathic fulgurite named *mazintarincan* in the *Lapidary* of King Alfonso X, from 1250), no exogenic fulgurites had been reported until modern times. To the best of the authors’ knowledge, Mohling in 2004 was the first to document the occurrence of an exogenic fulgurite south of the town of Elko, in Elko Hills, NE Nevada, USA, in 1997 (Fig. 1a) (Mohling, 2004). The second documented case, reported by Walter in 2008, occurred in Oswego, New York, USA (Fig. 1b) (Walter, 2011). The third documented occurrence was in August 2013 in a suburb of Dallas, Texas, USA (Fig. 1c).

In ancient Iberia, Celtiberians and Lusitanians revered a deity named Neto or Neton, the god of lightning, but it was the Romans who showed more religious veneration for places that had been struck by lightning bolts. It was a Roman practice to surround such sacred places with an enclosure open at the top (*puteal*) or to build a shrine (Macrobius and Kaster, 2011).

Tiedra (Valladolid, Castile and León, Spain) was built on the site of a pre-Roman town known as Amallobriga, subsequently settled by the Romans. At the Cerro de la Ermita archaeological site there is a religious building erected in honour of Our Lady of Tiedra Vieja that retains the Roman custom of making votive offerings. Religious amulets and abundant Hispano-Roman

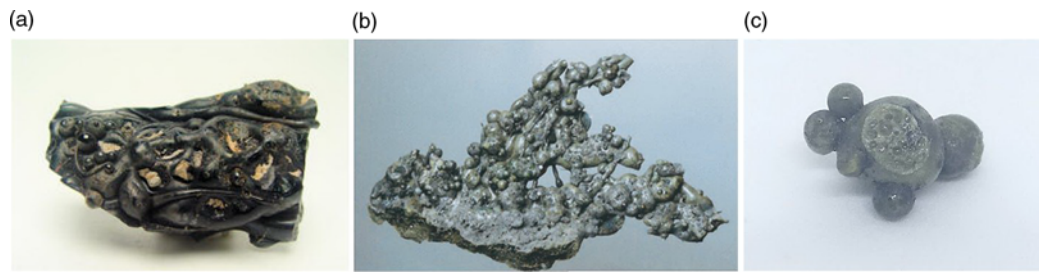


Fig. 1. (Colour online) Exogenic fulgurites from (a) Elko Hills, Nevada, (b) Oswego, New York, and (c) Dallas, Texas, USA.

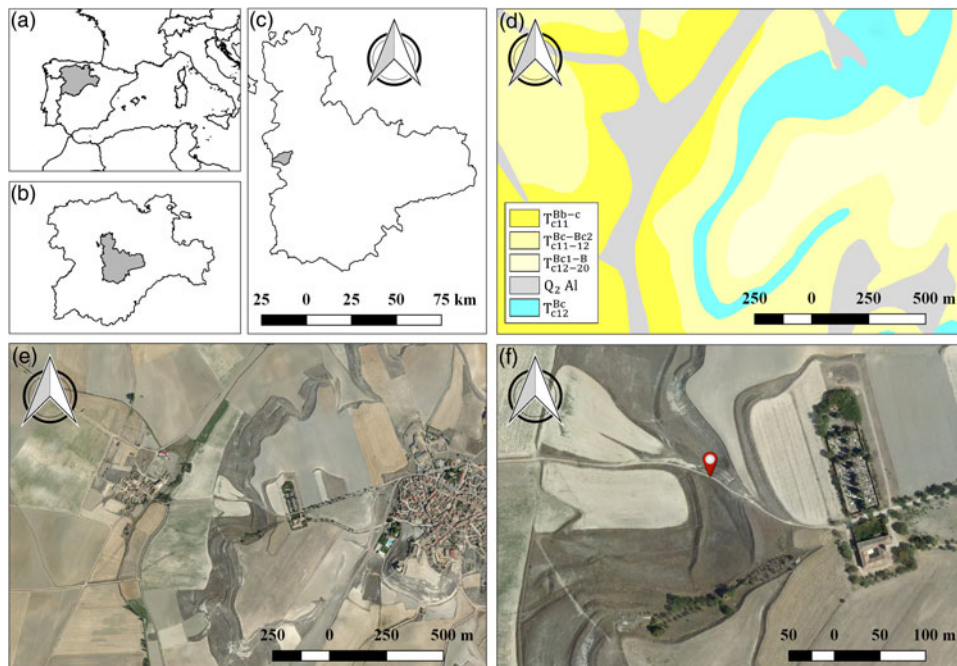


Fig. 2. (Colour online) (a–c) Location of Tiedra (Valladolid, Castilla y León, Spain); (d) geological map of Tiedra; (e) orthophoto of the same area shown in the geological map; (f) place of occurrence of the exogenous fulgurites (red marker; 41.6521978° N, 5.274904° W), on the Roman road to Pobladura de Sotiedra. Credit for the geological map: Spanish Geological Survey (IGME). Credit for the orthophotos (Spanish National Plan for Aerial Orthophotography, PNOA): Spanish National Geographic Institute (IGN). Geological map code: $c_{11}T^{Bb-c}$ = brown-grey and reddish-brown clays and silts with beds of sandstones ('Tierra de Campos Facies'), Miocene epoch, Spanish National Plan for Aerial Orthophotography, lowermost Vindobonian stage; $c_{11-12}T^{Bc-Bc2}$ = grey clays and white marls with intercalations of limestone and sandstone ('Cuestas Facies'), Miocene epoch, uppermost Vindobonian and Pontian stages; $c_{12-20}T^{Bc1-B}$ = recrystallized compact limestones ('Páramos Facies'), Pliocene epoch, Pontian stage; $c_{12}T^{Bc}$ = white marly limestones, Miocene epoch, Pontian stage; $Q_2 Al$ = sands, clays and alluvial gravel, Holocene epoch.

pottery have been discovered around the hermitage (Martín-Gil and Martín-Gil, 2001; Sanz-Mínguez and Sobrino-González, 2013). Along with these remains, intriguing droplets and vitrified masses were also found, which were initially misinterpreted as archaeologically anomalous material and discarded. In this study, their appropriate characterization as fulgurites, in accordance with the primitive sacred origin granted to the place, is reported. It is worth noting that the droplets investigated in this work showed no evidence of magnetic behaviour, thus ruling out the possibility of their being iron foundry slags.

This is the first report on exogenic fulgurites in Spain, given that a thorough search of the relevant literature yielded only two related articles in the Iberian peninsula, one on a natural fulgurite found in Bustarviejo, Madrid, Spain (García-Guinea *et al.*, 2009), and the other on a fulgurite generated by a small electricity pylon in Torre de Moncorvo, Bragança, Portugal (Martín Crespo *et al.*, 2009), neither of which were type-V.

2. Experimental

2.a. Location

The samples under study were found near the Roman road from Tiedra to Pobladura de Sotiedra (41.6521978° N, 5.274904° W), as shown in Figure 2, in September 1988.

The geology of the surrounding area comprises layers of sand and clays classified into the Neogene period, Miocene epoch, Tortonian stage (Vindobonian) (Fig. 2d). The dominant mineral species are quartz, kaolinite, muscovite and calcite. For a thorough mineralogical and petrological study of the site, the interested reader is referred to the work by Jiménez Fuentes and García Marcos (1980).

2.b. Materials

The area in which the fulgurites were found was an agricultural plot with a topsoil layer rich in ashes. The samples were located at a

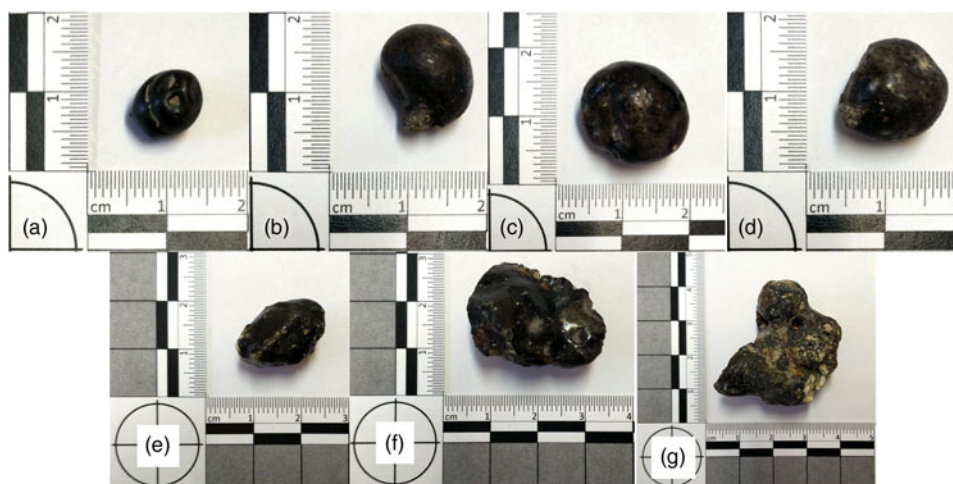


Fig. 3. (Colour online) Top row: droplets spewed (i.e. ejected) from the soil, which constitute the actual exogenic fulgurites. Samples were labelled as: (a) 'fulg1' (b) 'fulg2' (c) 'fulg3' and (d) 'fulg4'. In their original format they would have been attached to the matrix by very thin glass filaments (see the peduncle in 'fulg2'). Bottom row: Lightning-bolt induced vitrified composites (agglomerates), which can be regarded as pieces of the exofulgurites-matrix from which the droplet-like fulgurites were spewed. Samples were labelled as: (e) 'fulg5', (f) 'fulg6' and (g) 'fulg7'.

depth of several centimetres before being removed by a mould plough. They were protected by finely divided material. Their morphology suggests that they had barely experienced erosion and transport since their fragile surface was well preserved. The only appreciable deterioration, compared to recent fulgurites, was the loss of the peduncles, which may have occurred when they were unearthed. In fact, another fulgurite found within the contents of the ash altar at the temple of Lykaian Zeus at Mount Lykaion in Greece (Romano and Voyatzis, 2010) also appeared as well conserved as the ones reported herein.

The droplet-like exogenic fulgurites (Fig. 3a) showed a grey-green hue and ranged in size from 0.7 to 1.5 cm. All featured smooth, lustrous surfaces on all sides, suggesting that they had solidified in the air. None of them floated in water.

Apropos of the masses of the molten glass pieces (composites, Fig. 3b) close to the effusive centre, they showed vesicular bodies to which the droplets must have been attached. These 'exogenic fulgurite-matrix' pieces showed the vitreous aspect of droplets on their outer surface but their interior appeared as a heterogeneous mixture with fully differentiated components (phases or regions), which could be visually distinguished from one another: one of greenish appearance, one of brown hue and another entirely white. A small sample of the outer surface of one of these pieces was subjected to a carbon, hydrogen and nitrogen (CHN) analysis. The rest of the analyses were conducted using non-destructive techniques, given the categorization of the specimens as archaeological objects. Inner and outer parts of these samples are indicated as *i* (interior) and *e* (exterior), respectively.

2.c. Methods

Given the impossibility of grinding the samples to a fine powder to prepare KBr pellets, the vibrational spectra were first characterized using a Thermo Scientific (Waltham, MA, USA) Nicolet iS50 Fourier-Transform Infrared (FTIR) spectrometer equipped with an inbuilt diamond attenuated total reflection (ATR) system. The spectra were collected in the 400–4000 cm^{-1} region at room temperature with a 1 cm^{-1} spectral resolution; 64 scans were co-added and the resulting interferogram was averaged. The ATR-FTIR spectra were corrected using the advanced ATR

correction algorithm (Nunn and Nishikida, 2008) available in the OMNIC™ software suite.

FT-Raman spectra in the 4000–50 cm^{-1} range, at 3 cm^{-1} spectral resolution, were acquired also on non-ground samples with a micro-Raman spectroscopy system. A Horiba (Kyoto, Japan) T64000 apparatus, with focal length 0.64 m, $f/7.5$ aperture, diffraction gratings with 1800 gr mm^{-1} , single channel detection (with a R943 photomultiplier), and a N_2 -cooled 1" charge-coupled device (CCD) detector with 1024 × 256 pixels, was used. The 1064 nm line of Nd:YAG laser was used as excitation source and laser power was set at 100 mW. Images were taken with an Olympus BH2 (Shinjuku, Tokyo, Japan) microscope.

The X-ray powder diffractograms of the samples were obtained using a Bruker (Billerica, MA, USA) D8 Advance Bragg–Brentano diffractometer, in reflection geometry, with $\text{CuK}\alpha$ ($\lambda = 1.54 \text{ \AA}$) radiation and using crystalline silicon as a standard. X-ray generator: 40 kV, 40 mA; 1D LynxEye detector; scan mode: continuous PSD fast; $2\theta = 5\text{--}80^\circ$, in 0.02° steps, 1 s/step. Diffractograms were analysed in DIFFRAC.SUITE EVA software, using the most up-to-date ICDD (International Centre for Diffraction Data) and COD (Crystallography Open Database) databases for peak identification. It should be clarified that, since the archaeological specimens could not be ground to a fine powder, samples had to be mounted in such a way that the exposed surface would be as flat as possible (at the expense of reducing the intensity of low-angle peaks and adding noise to the diffractograms, which prevented subsequent Rietveld refinement).

Major (except Na and C) and minor elements were determined on non-ground samples by using a Niton XL3t XRF Analyzer (Thermo Fisher Scientific), using the TestAll™ Geo mode for a rapid analysis of major and trace elements (i.e. an overall composition of the sample). X-ray tube: Au anode, 50 kV, 200 μA . Data were processed using the Niton Data Transfer (NDT™) PC software suite.

C content in the outer layer of one of the 'matrix' samples was determined by dry combustion in a CHN-2000 Analyzer (LECO Corp., Saint Joseph, MI, USA). The sample was placed in a tared tin capsule and weighted using a microbalance. The combustion temperature was set to 950 °C and ethylenediaminetetraacetic acid (CAS 60-00-4, Sigma Aldrich, $\geq 99\%$) was used as the analytical standard.

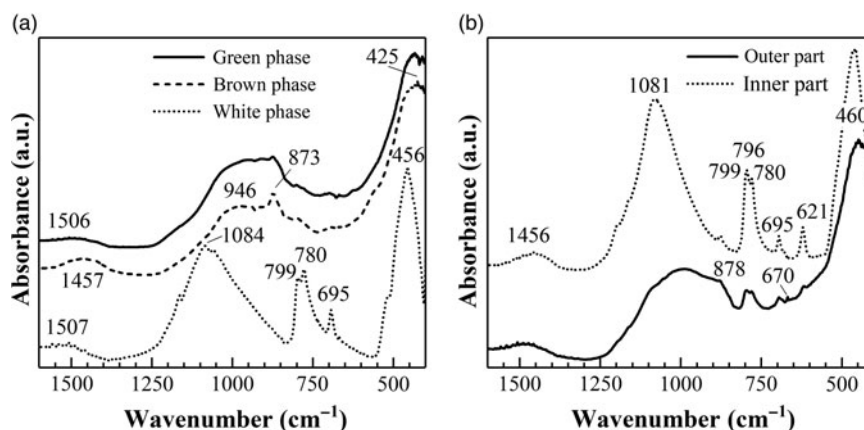


Fig. 4. Medium- and low-wavenumber regions in the ATR-FTIR spectra of: (a) green, brown and white phases in the lightning-bolt induced vitrified composites (fulg5); (b) inner and outer part of a droplet fulgurite (fulg1).

FTIR and CHN analyses were conducted at LTI-Palencia (Universidad de Valladolid, Spain), X-ray powder diffraction (XRPD) at the TAIL-UC facility (Universidade de Coimbra, Portugal), Raman spectroscopy at the Química-Física Molecular Research Unit lab (Universidade de Coimbra, Portugal), and X-ray fluorescence (XRF) at the GeoSciences Centre (Universidade de Coimbra, Portugal).

3. Results

3.a. Vibrational characterization

3.a.1. Infrared spectroscopy

In the molten glass-matrix composites (Fig. 4a), greenish and brown phases shared FTIR bands at 946, 873 and 425 cm⁻¹. The first band, at 946 cm⁻¹, is characteristic of silicate and aluminate glasses containing calcium. The second band, at 873 cm⁻¹, can be attributed either to a Si–N bond, to calcite (CaCO₃), or to C₆₀ or C₅₉N fullerenes, present in other fulgurites reported in the literature (Daly *et al.*, 1993; Heymann, 1998). The third band, at 425 cm⁻¹, may be assigned to any magnesium carbonate (magnesite, MgCO₃ or other minerals of the magnesite–siderite series, MgCO₃ to FeCO₃) (Brusentsova *et al.*, 2010). The greenish phase showed a weak band at 1506 cm⁻¹ that can be attributed either to a ν_3 carbonate vibration (Saikia *et al.*, 2008) or to a C–C stretching in an aromatic ring. The brown phase is characterized by a band at 1457 cm⁻¹ from either a C₅₉N azafulleren or a pressure-induced phase pC₆₀.

The white phase (also depicted in Fig. 4a) showed FTIR bands at 1084 cm⁻¹ (cristobalite, SiO₂), at 456 cm⁻¹ (attributed to the shock compressed quartz, lechatelierite, SiO₂) and the characteristic peaks for quartz (doublet at 799 and 780 cm⁻¹ and singlet at 695 cm⁻¹) (Foster and Walker, 1984). The absorption peaks at 780–800 cm⁻¹ are due to Si–O–Si symmetrical stretching vibration (tetrahedral–tetrahedral ion vibrations), and the absorption peak at 695 cm⁻¹ (Si–O–Si symmetrical bending vibration) arises due to octahedral site symmetry (Parthasarathy *et al.*, 2001; Saikia *et al.*, 2008). The two bands (not shown in Fig. 4a) that appeared at 2360 and 2342 cm⁻¹ correspond to the absorption doublet of CO₂.

The FTIR spectrum of the inner part of the droplet-fulgurites (Fig. 4b) showed bands at 1456 cm⁻¹ (compatible with N-doped graphene or fullerene allotropes C₆₀ and C₅₉N), at 1081 cm⁻¹

(Si–O–Si asymmetrical stretching vibration from quartz), at 796 cm⁻¹ (Si–O–Si symmetrical stretching vibration for cristobalite), at 780 and 799 cm⁻¹ (Si–O–Si symmetrical stretching vibration for quartz), at 695 cm⁻¹ (quartz), at 621 cm⁻¹ (cristobalite) (Foster and Walker, 1984) and at 460 cm⁻¹ (biotite, K(Mg, Fe)₃(AlSi₃O₁₀)(F,OH)₂; or phlogopite, KMg₃(AlSi₃)O₁₀(OH)₂). The doublet of CO₂ also appeared at 2360 and 2342 cm⁻¹ (not shown).

The outer crust of the droplets (Fig. 4b) shared several bands with the spectrum of the inner part (those arising from cristobalite and quartz), and showed additional weak bands at 878 cm⁻¹ (attributable to CaCO₃, vaterite or calcite), at 680 cm⁻¹ (pyroxenes such as hedenbergite, FeCaSi₂O₆; diopside, MgCaSi₂O₆; or augite (Ca,Na)(Mg,Fe,Al,Ti)(Si,Al)₂O₆), at 670 cm⁻¹ (magnetite feature), and at 406 cm⁻¹ (polaronic torsion in C–N–C bonds). The 2360 and 2342 cm⁻¹ doublet of CO₂ (not shown) was also present.

A probable feature during a lightning strike is that silicon in quartz is reduced to silicon metal, but in the exogenic fulgurites studied herein the typical phonon line of silicon at 520 cm⁻¹ and the band at 970 cm⁻¹ (related to disorder in a glass matrix) were not detected by FTIR. Other unique species to fulgurites, including silicides such as nauquite (previously named fersilicite, FeSi) and silicon carbide (SiC), and phosphides in the form of schreibersite (Fe₃P (Fe,Ni)₃P) and TiP (Sheffer *et al.*, 2003), were not detected either with this characterization technique, but will be discussed in subsequent sections.

3.a.2. Raman spectroscopy

For the outer part of the lightning-bolt induced vitrified composites, weak Raman lines were recorded at 320, 395 and 670 cm⁻¹ (diopside and augite), at 1015 cm⁻¹ (hedenbergite), and at 1120 cm⁻¹ and 1606 cm⁻¹ (hydrocarbons, C–C asymmetric stretching and C=C stretching, respectively (Carter *et al.*, 2010a, b)) (Fig. 5a). The inner part (Fig. 5b) showed weak lines in the 400–2750 cm⁻¹ region at 488 cm⁻¹ (S–S disulphide), at 1295 cm⁻¹ (polyenic chains), at 1442 cm⁻¹ (compatible with C₇₀ (Jeoung *et al.*, 1995)), at 1467 cm⁻¹ (compatible with C₆₀ (Lefrant *et al.*, 1993) and amorphous diamond (Prawer *et al.*, 1998)), at 2444 cm⁻¹ (compatible with graphite (Essene and Fisher, 1986)) and at 2730 cm⁻¹ (compatible with graphite), in addition to a sharp multiple band attributed to unidentified hydrocarbon molecules with peaks at 2852 cm⁻¹ (C–H₂ symmetric

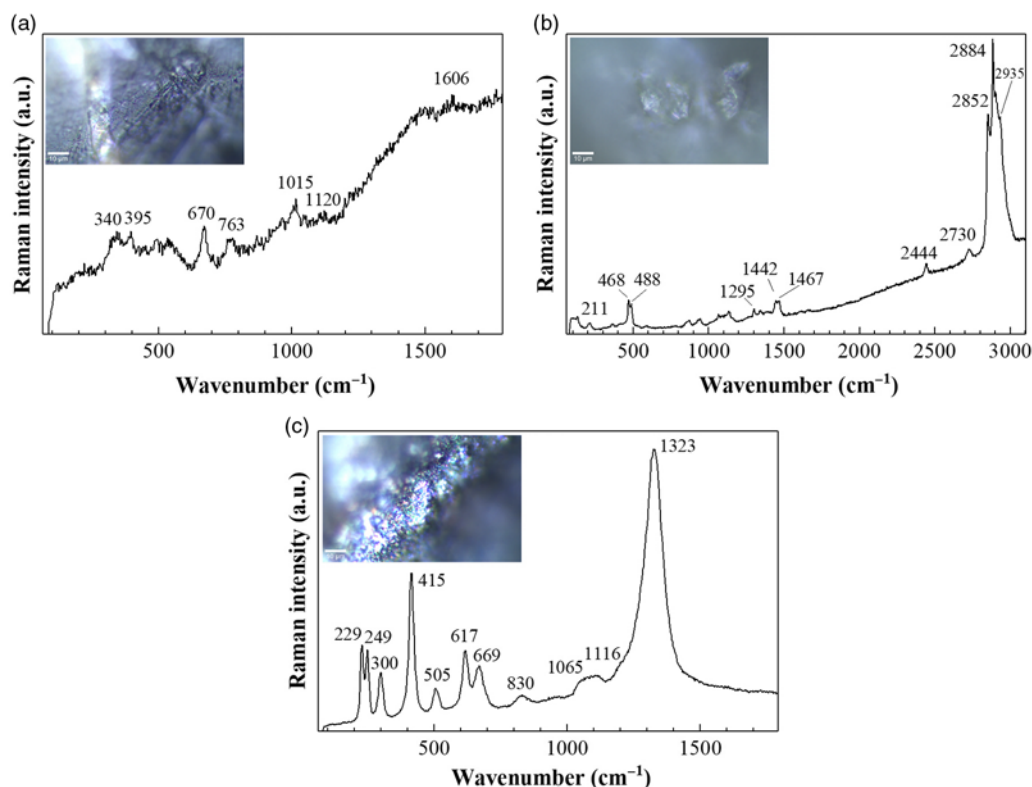


Fig. 5. (Colour online) Raman spectra of: (a) the outer surface and (b) the interior of the lightning-bolt induced vitrified composites (fulg5); (c) outer surface of a droplet-fulgurite (fulg1).

and asymmetric, respectively), at 2884 cm^{-1} (CH_3 symmetric stretching) and at 2935 cm^{-1} ($-\text{CH}_2$ and $-\text{CH}_3$) (Fig. 5b).

For the droplet-fulgurites (Fig. 5c) a series of sharp Raman lines were observed at 249 cm^{-1} (A_g mode, FeSi_2), 229 cm^{-1} and 415 cm^{-1} (cristobalite), at 300 and 617 cm^{-1} (tentatively ascribed to silicon (Temple and Hathaway, 1973)), at 505 cm^{-1} (albite), at 669 cm^{-1} (pyroxenes), at 830 cm^{-1} (graphitic structures), at $c. 1065\text{ cm}^{-1}$ (carbonates), at 1116 cm^{-1} (muscovite) and at 1323 cm^{-1} (graphite (Bokobza *et al.*, 2015)).

3.b. X-ray powder diffraction

In the diffractogram of the outer part of the matrix composites (grey-green glassy phase), and specifically in sample fulg5e, characteristic patterns for diopside (COD 9005340), augite (COD 1200006), hedenbergite (COD 9010328) and quartz (COD 1011176) could be observed (Fig. 6a). In the inner part of the same sample (white phase, sample fulg5i) cristobalite (COD 9008226), quartz (COD 9012600) and calcite (COD 1010962) were identified (Fig. 6b). For the outer surface of fulg6 matrix composite, peaks associated with magnesioferrite ($\text{Mg}(\text{Fe}^{3+})_2\text{O}_4$, COD 9001469), diopside and, in smaller quantities, maghemite ($\gamma\text{-Fe}_2\text{O}_3$, PDF 39-1346), hercynite ($\text{Fe}^{2+}\text{Al}_2\text{O}_4$, COD 9013623), mcgovernite ($\text{Mn}_{19}\text{Zn}_3(\text{AsO}_4)_3(\text{AsO}_3)(\text{SiO}_4)_3(\text{OH})_{21}$, PDF 25-0531) and silicon carbide (PDF 02-1462) were indexed.

Maghemite presence was evidenced in fulg1 droplet fulgurite by peaks at 2θ angles of 30° (220), 36° (311), 43° (400) and 57° (511) (Fig. 6d). The absence of peaks at $2\theta = 10.5^\circ$, 17° and 20.5° questioned the presence of C_{60} postulated from FTIR, but magnesioferrite, naquite silicide or fersilicite (PDF 38-1397) and silicon carbide, not identified by FTIR, were found. The diffraction pattern

for outer surface of fulg2 (Fig. 6e) resembled those of fulg5e and fulg6e, with diopside, magnesioferrite and quartz as the main mineral components.

3.c. Elemental analyses

Proportions of elements (in wt %), determined by XRF, are summarized in Table 1. The high Fe proportion for sample fulg1 was in good agreement with the composition based on magnesioferrite, naquite (fersilicite) and maghemite identified by XRPD. Combinations of Si/Al, Si/Fe and Si/Mg with values of around 5.0, 3.7 and 23.0 for sample fulg2 lead to a bulk assignment to diopside, augite and magnesioferrite. Composition of samples fulg3, fulg4 (not studied by other techniques) and fulg5e (studied by FTIR, Raman and XRPD) were also compatible with pyroxenes. Fulg6 exhibited Ca and Si percentages similar to those of fulg2. It is worth noting that Fulg4 exhibited a relatively high Zr content (0.17 %).

As regards C content, a CHN analysis was carried out for the outer crust of one of the 'matrix' samples (Fulg5e), obtaining C, H and N percentages of 1 %, 0.2 % and 0.2 %, respectively. This composition is compatible with carbonaceous materials based in elemental forms and allotropes of elemental carbon such as graphite, C_{60} and carbon black.

4. Discussion

The pressure and temperature conditions during lightning strikes are extreme and exceed the capabilities of the equipment available in synthesis laboratories, making it impossible to reconstruct how the components in fulgurites are formed (in spite of the efforts to

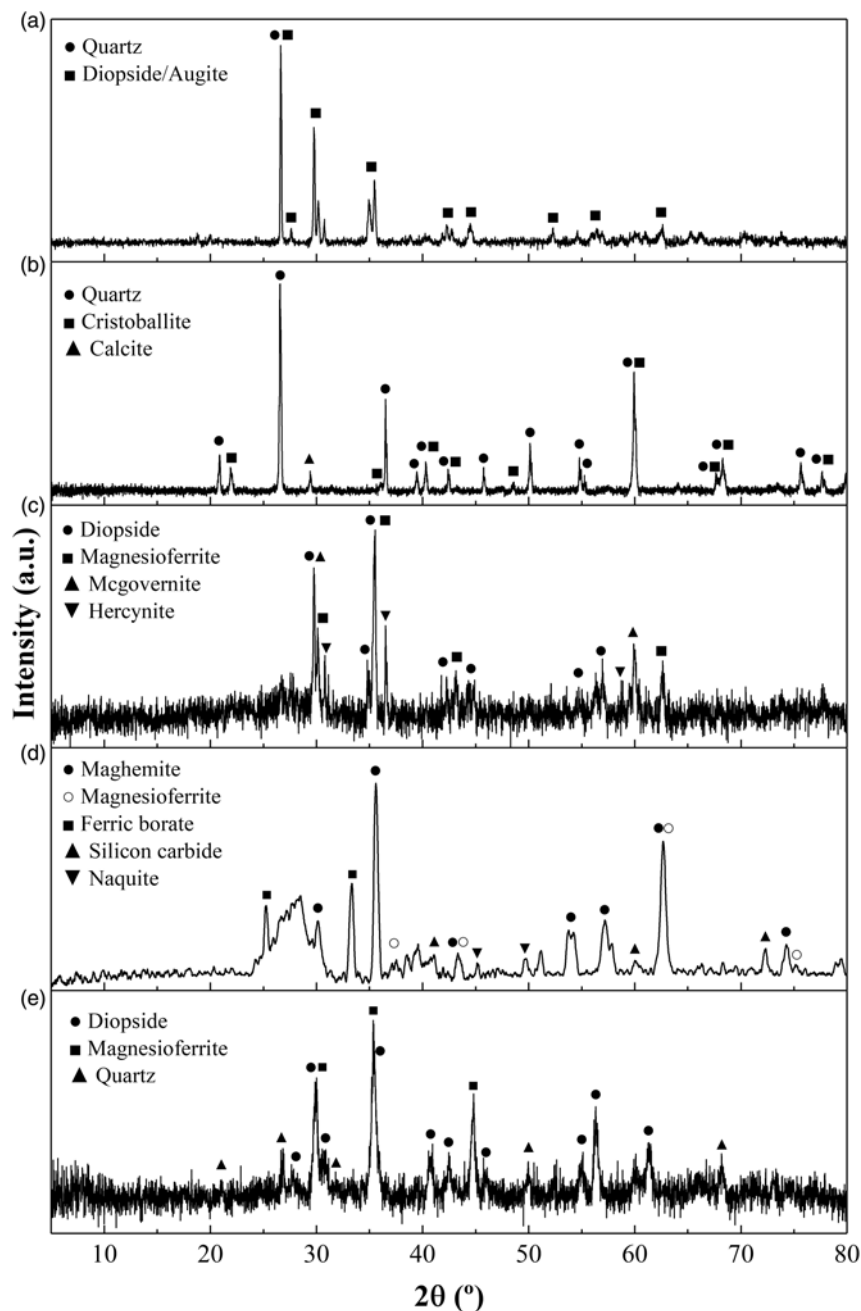


Fig. 6. XRPD patterns for: (a) exterior and (b) interior of one of the lightning-bolt induced vitrified composites (fulg5e and fulg5i, respectively); (c) outer surface of another vitrified composite (fulg6e); (d–e) outer surface of two of the droplet-fulgurites (fulg1 and fulg2, respectively).

reproduce the process by using, for instance, laser ablation (Martínez-Ramírez *et al.*, 2013)). What is known is that, in a rapid discharge, which occurs in a lightning bolt, the thermal energy is first consumed by vaporizing and melting the soil and subsequently diffuses radially outward from the spark where it melts and *bakes* the soil (Pasek and Pasek, 2017).

The presence of amorphous quartz in the composition for the white phase in the exogenic fulgurite-matrix aggregates suggests that the abrupt electrical (Joule) heating of the soil surface yields high temperatures, which produces a thin melt layer on the surface, which then cools adiabatically. Cristobalite was found in the presumably hotter regions of the fulgurite, adjacent to the glassy melt.

The cooling of the melted glass would take place in the ozonized atmosphere thereby developed and would give rise to a *baked* glass that appears as a dark crust in the outer part of the pieces of the matrix and in the droplets that were spewed. The glass showed a composition of pyroxene, iron oxide and silicides. The low presence of carbonaceous materials in the glass suggests a high pyrolysis temperature induced in organic substances and a rapid quenching of the melt-trapped CO_x gases produced during heating (see Carter *et al.*, (2010a, b) and references therein).

The core, or inner part, of the exofulgurites was found to be richer in cristobalite, while the composition of the outer parts showed higher diopside, maghemite and albite contents and more

Table 1. Elemental composition by weight percent (wt %) for Tiedra exogenic fulgurite samples: main (top) and minor (bottom) constituents

Sample	Fe	Mn	Ti	Al	Ca	K	Si	Mg	P	Mineral										
fulg1	75.52		0.22	4.18	7.44	1.44	9.40		0.45	Magnesioferrite, maghemite, naquite										
fulg2	12.06	0.15	0.85	9.18	16.50	8.00	49.64	2.10	0.62	Diopside, augite and magnesioferrite										
fulg3	14.90	0.18	0.70	7.98	10.66	9.37	54.91		0.55	Pyroxenes (hedenbergite)										
fulg4	9.22	0.16	1.95	10.95	7.03	10.20	55.19	3.34	1.08	Pyroxenes (augite and diopside)										
fulg5e	25.00	0.19	0.47	6.07	18.85	3.74	42.64	1.70	0.55	Pyroxenes (augite and diopside)										
fulg5i	13.34	0.44	0.47	6.11	11.97	3.63	62.01		1.85	Quartz and cristoballite										
fulg6e	26.94	0.57	0.49	5.99	16.35	5.70	43.13		0.55	Magnesioferrite and diopside										
Sample	Sb	Sn	Cd	Pd	Nb	Zr	Bi	Pb	Zn	Cu	Ni	Cr	V	Sr	Rb	As	Sc	Cs	Te	Cl
fulg1						0.01		0.14	0.01	0.05	0.03		0.03	0.02		0.05	0.03	0.03	0.03	0.26
fulg2	0.01	0.01				0.06				0.01	0.03	0.07	0.03	0.07	0.01	0.01	0.04	0.02	0.02	0.10
fulg3	0.01					0.05			0.01	0.01	0.03	0.06	0.03	0.06	0.01	0.01	0.07	0.02	0.02	0.16
fulg4						0.10		0.01	0.01	0.01	0.01	0.04	0.03	0.04	0.02			0.01	0.01	0.24
fulg5e						0.02				0.01	0.01	0.13	0.03	0.02			0.05	0.04	0.07	0.03
fulg5i						0.05			0.01	0.01	0.02	0.04	0.02	0.02	0.01	0.01		0.01		0.03
fulg6e						0.06			0.01	0.01	0.03	0.10	0.03	0.03	0.01	0.01	0.06	0.03	0.04	0.04

zirconium. This variation could be due to a number of reasons, including the melting processes.

Although the exogenic fulgurites found in the archaeological site of Tiedra share some components (shocked quartz and cristobalite) with the quartzofeldspathic fulgurites found in Bustarviejo (García-Guinea *et al.*, 2009), they do not contain the Si–Fe–Al alloys present in the latter. Naquite, iron oxides, silicon carbide and pyroxenes were identified instead. The comparison with the composition of exogenic fulgurites from Elko Hills and Oswego has not been performed due to lack of data (their discoverers have not yet published any chemical analysis results). With regard to the comparison with the Texas exogenic fulgurites, in spite of the similarities in terms of appearance, there were substantial differences in terms of composition: in our preliminary analyses of one of the Dallas fulgurites (their discoverer has not yet studied them in detail) we have found quartz, calcite, feldspars and iron oxides, but not unique species such as naquite, schreibersite, SiC or TiP.

The presence of buckminsterfulleren, C₆₀ (a naturally occurring molecule produced when a lightning bolt strikes a hardwood tree) and other carbon compounds such as graphite, reported by other authors (Essene and Fisher, 1986; Daly *et al.*, 1993; Frank *et al.*, 2006), albeit suggested on the basis of the FTIR and Raman spectra of the samples reported herein, could not be confirmed by XRPD.

Correlation between results has been carried out through a concordance analysis based on the score of the number of matches (3, 2 or 1) for the mineral species that appeared in the identification profiles obtained through each of the techniques and taking into account their elucidative power (XRD > Raman = FTIR = XRF). Accordingly, the presence of cristobalite and pyroxenes (such as diopside, hedenbergite and augite) would be a substantiated and clear result (three occurrences); quartz/lechatelierite, maghemite, diopside, magnesioferrite, naquite and C₆₀ or C₅₉ may be regarded as components present with a high degree of certainty (two occurrences); and calcite, albite, moscovite, biotite, phlogopite, graphite and CO₂ can be deemed as suggested components (one occurrence).


Apropos of the samples' dating, it should be clarified that, although there is no certainty on the fact that the fulgurites under study date from Roman times, there is a high probability, provided that they were found along with many fragments of *terra sigillata hispanica*, and without contamination from modern remains. All the findings appeared in an area of 2 m × 2 m.

Finally, in regard to the association between sacred archaeological sites and vitrified materials, previously reported for vitrified stones in some dolmen (Abrunhosa *et al.*, 1995) and for the circular stone enclosures of the Iron Age known as *vitrified hill-forts* (Cook *et al.*, 2014), it would be further supported from the finding of glassy exogenic fulgurites in this Roman archaeological site.

5. Conclusions

The characterization of exogenic fulgurites found in the archaeological site of Tiedra represents the first study on Spanish exogenic fulgurites to date. The droplet fulgurites reported herein can be described as quartzo-pyroxene materials the composition of which includes naquite and CSi silicides; pyroxenes such as augite, diopside and hedenbergite; iron oxides such as maghemite and magnesioferrite; shocked quartz and neofomed cristobalite. Highly vesicular bodies and droplets are compatible with the siliclastic sands (Tortonian) in the area.

The presented mineralogical and chemical data may help to shed light on high-temperature processes in geological systems and dynamic rock transformation in ultrafast events, and may be useful for gaining an insight into fulgurite glass formation processes.

Author ORCIDs.  Pablo Martín-Ramos, 0000-0003-2713-2786; Francisco PSC Gil, 0000-0001-7546-0288; Francisco J Martín-Gil, 0000-0003-4989-6197; Jesús Martín-Gil, 0000-0001-9921-2465

Acknowledgements. Access to the TAIL-UC facility funded under the QREN-Mais Centro project ICT-2009-02-012-1980 and to the GeoSciences Centre of the Department of Earth Sciences XRF equipment at FCTUC (Prof. Lidia M. Gil

Catarino) is acknowledged. P.M.R. acknowledges the financial support of Santander Universidades through the 'Becas Iberoamérica Jóvenes Profesores e Investigadores, España' scholarship programme. Dr Melissa Boyd is gratefully acknowledged for her diligent proofreading of this paper.

Declaration of interest. The authors declare no conflict of interest.

References

- Abrunhosa MJ, Gonçalves AA & da Cruz DJ** (1995) Occorrência de rochas vitrificadas no dólmen do "Picoto do Vasco" (Vila Nova de Paiva, Viseu). *Estudios Pré-Históricos* **3**, 167–85.
- Bokobza L, Bruneel J-L & Couzi M** (2015) Raman spectra of carbon-based materials (from graphite to carbon black) and of some silicone composites. *C* **1**, 77–94.
- Brusentsova TN, Peale RE, Maukonen D, Harlow GE, Boesenberg JS & Ebel D** (2010) Far infrared spectroscopy of carbonate minerals. *American Mineralogist* **95**, 1515–22.
- Carter EA, Hargreaves MD, Kee TP, Pasek MA & Edwards HGM** (2010a) A Raman spectroscopic study of a fulgurite. *Philosophical Transactions of the Royal Society A: Mathematical, Physical and Engineering Sciences* **368**, 3087–97.
- Carter EA, Pasek MA, Smith T, Kee TP, Hines P & Edwards HGM** (2010b) Rapid Raman mapping of a fulgurite. *Analytical and Bioanalytical Chemistry* **397**, 2647–58.
- Cook M, Watson F & Cook G** (2014) Burning questions: new insights into vitrified forts. In *17th Iron Age Research Student Symposium* (eds GJR Erskine, P Jacobsson, P Miller and S Stetkiewicz), pp. 149–56. Edinburgh: Archaeopress Publishing Ltd.
- Daly TK, Buseck PR, Williams P & Lewis CF** (1993) Fullerenes from a fulgurite. *Science* **259**, 1599–601.
- Elmi C, Chen J, Goldsby D & Gieré R** (2017) Mineralogical and compositional features of rock fulgurites: a record of lightning effects on granite. *American Mineralogist* **102**, 1470–81.
- Essene EJ & Fisher DC** (1986) Lightning strike fusion: extreme reduction and metal-silicate liquid immiscibility. *Science* **234**, 189–93.
- Foster RD & Walker RF** (1984) Quantitative determination of crystalline silica in respirable-size dust samples by infrared spectrophotometry. *The Analyst* **109**, 1117–27.
- Frank O, Jehlička J & Hamplová V.** (2006) Search for fullerenes in geological carbonaceous samples altered by experimental lightning. *Fullerenes, Nanotubes and Carbon Nanostructures* **11**, 257–67.
- Gailliot MP** (2016) Petrified lightning. *Rocks & Minerals* **55**, 13–17.
- García-Guinea J, Furio M, Fernandez-Hernan M, Bustillo MA, Crespo-Feo E, Correcher V, Sanchez-Muñoz L, Matesanz E & Gucsik A** (2009) The quartzofeldspathic fulgurite of Bustaviejo (Madrid): cathodoluminescence and Raman emission. In *AIP Conference Proceedings* **1163**, Mainz, Germany, pp. 128–34.
- Heymann D** (1998) Search for C₆₀ fullerene in char produced on a Norway spruce by lightning. *Fullerene Science and Technology* **6**, 1079–86.
- Jeoung SC, Kim D, Kim S & Kim SK** (1995) Triplet state Raman spectra of C₆₀ and C₇₀. *Chemical Physics Letters* **241**, 528–32.
- Jiménez Fuentes E & García Marcos JM** (1980) *Explicación de la hoja nº 370: Toro (Zamora y Valladolid)*. Madrid: Instituto Geológico y Minero de España.
- Kassi AM, Kasi AK, Friis H & Kakar DM** (2013) Occurrences of rock-fulgurites associated with steel pylons of the overhead electric transmission line at Tor Zawar, Ziarat District and Jang Tor Ghar, Muslim Bagh, Pakistan. *Turkish Journal of Earth Sciences* **22**, 1010–19.
- Lefrant S, Faulques E, Godon C, Buisson JP, Auban-Senzier P, Jerome D, Fabre C, Rassat A, Zahab A, Lambert JM & Bernier P** (1993) Isotope effects in the Raman spectra of ¹³C enriched C₆₀. *Synthetic Metals* **56**, 3044–9.
- Macrobius AAT & Kaster RA** (2011) *Saturnalia*. Cambridge, MA: Harvard University Press.
- Martin Crespo T, Lozano Fernandez RP & Gonzalez Laguna R** (2009) The fulgurite of Torre de Moncorvo (Portugal): description and analysis of the glass. *European Journal of Mineralogy* **21**(4), 783–94.
- Martín-Gil J & Martín-Gil FJ** (2001) ¿Un fanum romano en Tiedra? *Investigación y Ciencia* **239**, 29. https://www.researchgate.net/publication/260426668_Hispania_Romana_Un_fanum_en_Tiedra
- Martínez-Ramírez S, Díaz L, Camacho JJ & Viehland D** (2013) CW CO₂-laser-induced formation of fulgurite on lime-pozzolan mortar. *Journal of the American Ceramic Society* **96**, 2824–30.
- Mohling JW** (2004) Exogenic fulgurites from Elko County, Nevada: a new class of fulgurite associated with large soil-gravel fulgurite tubes. *Rocks & Minerals* **79**, 334–40.
- Nunn S & Nishikida K** (2008) *Advanced ATR Correction Algorithm – Application Note 50581*. Madison, WI: ThermoScientific.
- Parthasarathy G, Kunwar AC & Srinivasan R** (2001) Occurrence of moganite-rich chalcidony in Deccan flood basalts, Killari, Maharashtra, India. *European Journal of Mineralogy* **13**, 127–34.
- Pasek MA, Block K & Pasek V** (2012) Fulgurite morphology: a classification scheme and clues to formation. *Contributions to Mineralogy and Petrology* **164**, 477–92.
- Pasek MA & Pasek VD** (2017) The forensics of fulgurite formation. *Mineralogy and Petrology* **112**, 185–98.
- Prawer S, Nugent KW & Jamieson DN** (1998) The Raman spectrum of amorphous diamond. *Diamond and Related Materials* **7**, 106–10.
- Romano DG & Voyatzis ME** (2010) Excavating at the birthplace of Zeus: the Mt. Lykaion Excavation and Survey Project. *Expedition: The Magazine of the University of Pennsylvania* **52**, 9–21.
- Saikia BJ, Parthasarathy G, Sarmah NC & Baruah GD** (2008) Fourier-transform infrared spectroscopic characterization of naturally occurring glassy fulgurites. *Bulletin of Materials Science* **31**, 155–8.
- Sanz-Mínguez C & Sobrino-González M** (2013) Tiedra: el cerro de la Ermita. *Vaccea* **2012** (no. 6), 26–31.
- Sheffer A, Melosh H, Jarnot B & Lauretta D** (2003) Reduction of silicates at high temperature: fulgurites and thermodynamic modeling. In *Lunar and Planetary Science Conference*, League City, Texas, pp. 1–2.
- Temple PA & Hathaway CE** (1973) Multiphonon Raman spectrum of silicon. *Physical Review B* **7**, 3685–97.
- Walter M** (2011) An exogenic fulgurite occurrence in Oswego, Oswego County, New York. *Rocks & Minerals* **86**, 264–70.